Numerical simulations of parity–time symmetric nonlinear Schrödinger equations in critical case

Edès Destyl, Jacques Laminie, S.P. Nuiro, Pascal Poullet

Numerical simulations of Parity–Time symmetric nonlinear Schrödinger equations in critical case

E. Destyl*, J. Laminie, S.P. Nuiro and P. Poullet
Laboratoire de Mathématiques Informatique et Applications (LAMIA),
Université des Antilles
BP 250, F-97157 Pointe à Pitre cedex, Guadeloupe FWI

May 14, 2020

Abstract

In this paper, we study the solution behavior of two coupled non–linear Schrödinger equations (CNLS) in the critical case, where one equation includes gain, while the other includes losses. Next, we present two numerical methods for solving the CNLS equations, for which we have made a comparison. These numerical experiments permit to illustrate other theoretical results proven by the authors [11]. We also obtain several numerical results for different non–linearities and investigate on the value of the blow up time relatively to some parameters.

Keywords

Numerical simulations, Blow up solution, Parity–Time symmetry, Nonlinear Schrödinger equations, Crank–Nicolson scheme, Finite difference method

Mathematics Subject Classification
35B40, 35B44, 35J10, 35Q41, 65M06, 68N15, 65N05

*Corresponding author. Email edes.destyl@univ-antilles.fr

Introduction

Various physical applications stimulate the interest to explore and study the solution behavior of systems of coupled nonlinear Schrödinger (CNLS) equations. Among them, one recovers several applications of nonlinear optics (birefringent optics fibers[1], filamentation, waves guided plasmonics, for example).

Hereafter, a basic model of propagation of weakly dispersive waves is considered by a system of the CNLS equations written as follows:

$$\left\{\begin{array}{rcl} \imath\partial_t u &=& -\Delta u + \kappa v + \imath\gamma u - (g_1|u|^2 + g|v|^2)u, \\ \imath\partial_t v &=& -\Delta v + \kappa u - \imath\gamma v - (g|u|^2 + g_2|v|^2)v, \\ (u(t=0), v(t=0)) &=& (u_0(x), v_0(x)), \quad x \in \mathbb{R}^d, \quad t = 0, \end{array}\right. \tag{1}$$

where the coefficients of the nonlinear parts are reals, the $\imath$ is the complex such that $\imath^2 = -1$ and the coefficients κ and γ are positives constants which characterize gain and loss in wave components and (u_0, v_0) is the initial condition. The system (1) can be viewed as a slight extension of that is considered by researchers in optics for which $g_1 = g_2$ is the self–phase modulation (SPM) and g is the cross–phase modulation (XPM) [17].

Let us recall that when the coefficients g_1 and g_2 are equal, the system (1) obeys the formal property called Parity–Time (PT) symmetry which means that if the pair $(u(x,t), v(x,t))$ is solution of the system (1), then the pair $(u_{PT}(x,t), v_{PT}(x,t)) = (\bar{v}(x,-t), \bar{u}(x,-t))$ is also solution of the same system (hereafter an overbar stands for the complex conjugation). This concept of PT–symmetry which emerged from quantum mechanics [6] (and references therein) has gained a particular relevance due to its importance in several areas of nonlinear Physics. Moreover, the behavior of the solution of system (1) is linked to the interaction between this property and the nonlinear potentiel. In the one dimension case, we have proven recently that as soon as the symmetry is unbroken ($0 < \gamma < \kappa$), the solution cannot blow up in finite time in H^1 norm, while if $\gamma \geq \kappa$ there exists a global solution that tends to infinity in L^2 norm (as soon as t tends to infinity) [7]. But in two dimension, this result is not so obvious. The nonlinearity terms seems to have more influence than PT–symmetry onto the solution behavior. Indeed, Dias et *al.* proved that in supercritical case ($d \geq 3$), the sufficient conditions of the existence of the finite time blow up does not rely on the PT–symmetry property [11]. In a recent paper, Dias et *al.* extended their result of the existence of the finite time blow up of solution to the critical case but only for $\kappa = 0$ and $\gamma > 0$ [12]. In our recent paper [9], sufficient conditions for the solution blow up have been obtained in two dimension case.

In this paper, a numerical study of the coupled system of nonlinear Schrödinger equations is made notably in the two dimension case, where, to our knowledge, the mathematical problems are still open. Recall that the system has a cubic nonlinearity, therefore, in the case of dimension 2, there is necessarily a L^2–critical dimension. In this case, the solution of the problem can be global or blow up in finite time. It should also be noted that this two–dimensional system has been partially approached in the particular case of a Manakov PT–symmetric system (see [19]). These authors have provided sufficient conditions that allow to obtain theoretical results on the overall existence and the blow up of the solution in finite time. To our knowledge, all the theoretical results already proved have never been illustrated by numerical simulations, and that also motivated us to propose some in this paper.

The main purpose of this work is to develop a numerical solver for the CNLS system (1) and to analyse the results. Although the original problem is defined on $\mathbb{R}^2$, the discret one

must be define on a open bounded domain without boundary conditions specified by Physics. In the case of a single NLS equation, several types of boundary conditions have been used, eg periodic boundary conditions, absorbing boundary conditions [13], perfectly matched layers (PML) [23], and transparent or exact boundary conditions ([3], [2]).

We consider initial conditions of Gaussian type centered at $(0,0)$ in a square domain $I =]-L,L[\times]-L,L[$. This constant L will be assumed large enough so that the contribution of the homogeneous Dirichlet boundary condition stays negligible. As soon as this last one is no longer, the maximum time of the simulation is achieved, and then the truncated solution of (1) is strongly affected by the boundary condition.

Thus, the chosen initial conditions are:

$$u_0(x,y) = Ae^{-(x^2+y^2)} \quad \text{and} \quad v_0(x,y) = Be^{-(x^2+y^2)} \tag{2}$$

with A and B are real constants.

Let us consider the density and the energy which characterize the solution:

$$Q(t) = \int \left(|u|^2 + |v|^2\right) dx$$

and

$$E(t) = \int \left(|\nabla u|^2 + |\nabla v|^2 + \kappa(\bar{u}v + u\bar{v}) - \frac{g_1}{2}|u|^4 - \frac{g_2}{2}|v|^4 - g|u|^2|v|^2\right) dx$$

For $\gamma = 0$, these quantities (for the Hamiltonian version) of the generalized Manakov equations (1) are conserved. Then, adding the product of the first equation times $2\bar{u}$ and the second by $2\bar{v}$, one obtains after integration in space, that the imaginary part of the expression leads to

$$\frac{dQ}{dt}(t) = 2\gamma \int \left(|u|^2 - |v|^2\right) dx.$$

Next, summing the product of the first equation by $2\partial_t\bar{u}$ and the second by $2\partial_t\bar{v}$, one obtains after integration in space, that the real part of the expression gives:

$$\frac{dE}{dt}(t) = 2\gamma \int \left(|\nabla u|^2 - |\nabla v|^2 - g_1|u|^4 + g_2|v|^4\right) dx.$$

We also define the H^1 semi–norm of the solution of the system (1) by

$$D(t) = \int \left(|\nabla u|^2 + |\nabla v|^2\right) dx.$$

For the next consideration, the introduction of the Stokes variables is needed in the explicit form,

$$S_1 = \int (\bar{u}v + u\bar{v})dx, \quad S_2 = \imath \int (\bar{u}v - u\bar{v})dx, \quad S_3 = \int (|u|^2 - |v|^2)dx.$$

In the Manakov case ($g_1 = g_2 = g$) and the PT–symmetry unbroken ($\gamma < \kappa$), using the derivative of previous quantities, one shows that the density is solution of a second order ODE [19, 7]. It can therefore be written in this new form

$$Q(t) = \frac{\kappa C}{\omega^2} + A_1 \cos(2\omega t) + A_2 \sin(2\omega t) \tag{3}$$

where

$$\omega^2 = \kappa^2 - \gamma^2, \quad C = \kappa Q(0) - \gamma S_2,$$

$$A_1 = Q(0) - \frac{\kappa C}{\omega^2}, \quad \text{and} \quad A_2 = \frac{1}{2\omega}\frac{dQ}{dt}(0).$$

This new expression provides an upper bound for the density:

$$Q(t) < Q_{\max}, \qquad \text{where} \quad Q_{\max} = \frac{\kappa C}{\omega^2} + \sqrt{A_1^2 + A_2^2}.$$

The paper is organized as follows. The first section describes the numerical methods and algorithm that have been implemented to solve the Cauchy problem. The next section addresses the error analysis of the scheme and the performance of the two methods that have been used. The numerical results using Gaussian beams as initial conditions for the PT–symmetric model are gathered in the third section. We end up with some concluding remarks and perspectives.

1 Numerical scheme

Let us denote by L and T, 2 positive real constants, the former being the half-length of the physical domain in 1D, the latter, a maximal time. The system (1) is then considered in a square domain $I =]-L, L[\times]-L, L[$ for $t \in [0, T]$. This square I is uniformly divided into a spatial grid of size $\delta x \times \delta y$ and the gridpoints are defined by $x_i = x_0 + i\delta x$ and $y_j = y_0 + j\delta y$, where $x_0 = y_0 = -L$.

Let δt be the time step, and (U^n, V^n) the approximate solution of the model (1) at time $t^n = n\delta t$. We get the following semi–discrete system using Crank–Nicolson scheme as follows:

$$\imath\left(\frac{U^{n+1}-U^n}{\delta t}\right) = -\Delta\left(\frac{U^{n+1}+U^n}{2}\right) + \imath\gamma\left(\frac{U^{n+1}+U^n}{2}\right) + \kappa\left(\frac{V^{n+1}+V^n}{2}\right) - \Theta(g_1, g, U^{n+1}, U^n, V^n) \quad (4)$$

$$\imath\left(\frac{V^{n+1}-V^n}{\delta t}\right) = -\Delta\left(\frac{V^{n+1}+V^n}{2}\right) - \imath\gamma\left(\frac{V^{n+1}+V^n}{2}\right) + \kappa\left(\frac{U^{n+1}+U^n}{2}\right) - \Theta(g_2, g, V^{n+1}, V^n, U^n) \quad (5)$$

with $\Theta(a, b, c, d, e) = \frac{1}{2}\left(a(|c|^2 c + |d|^2 d) + b|e|^2(c + d)\right)$.

Let us denote by $(U^n_{i,j}, V^n_{i,j})$ the value of (U^n, V^n) at the point (x_i, y_j) for the time t_n. By using second order centered finite differences, the Laplacian terms are approximated by :

$$-(\Delta U^n)(x_i, y_j) \approx \frac{1}{\delta x^2}\Big(2U^n_{i,j} - U^n_{i+1,j} - U^n_{i-1,j}\Big) + \frac{1}{\delta y^2}\Big(2U^n_{i,j} - U^n_{i,j+1} - U^n_{i,j-1}\Big) \quad (6)$$

These discrete Laplacian terms (6) with the discrete values allow to obtain the full nonlinear system from (4) and (5). Two solvers are considered to solve this coupled non linear system: a fixed point iteration that is combined with a splitting between the two equations [10], and the Newton method (see hereafter).

In fact, at each time step, one uses an inexact Newton method, which consists of seeking the solution of the nonlinear system of equations:

$$F(W) = \begin{pmatrix} F_1(W) \\ F_2(W) \end{pmatrix} = \begin{pmatrix} 0 \\ 0 \end{pmatrix}, \quad \text{with} \quad W = \left(U^{n+1}, V^{n+1}\right).$$

By assuming that F is $\mathbb{C}^{2N_xN_y}$-differentiable and the Jacobian $DF(W)$ is regular, a sequence $(W_k)_{k\geq 0}$ is defined recursively by,

$$\begin{cases} W_0 = (U^n, V^n) \\ W_{k+1} \quad \text{is the solution of} \quad DF(W_k)(W_{k+1} - W_k) = -F(W_k), \quad k \geq 0. \end{cases}$$

The inner linear systems are solved by GMRES algorithm for complex-valued functions, and the sequence $(W_k)_{k\geq 0}$ converges to (U^{n+1}, V^{n+1}), the root of the nonlinear complex function.

2 Program implementation and validation

In this section, we wish to testify to all the attention that has been paid to build our solver. First of all, specific care must be made to chose the programming language that is suitable to our algorithm implementation. To combine the flexibility of a language and the performance of the application is most of time impossible in a simply way. So, one proposes a multi–language implementation using an interpreted language (Python) and a compiled one (Fortran). Therefore, the characteristics of these two languages are mixed, in order to create a robust and efficient application via C language interfaces. Both languages have a standard way to write C–interfaces, ctype in Python (a part of Numpy library) and C binding in Fortran.

In order to compare the two iterative methods, as no analytical solution exists, one uses a referent solution computed with very fine mesh $\delta x = \delta y = 2 \times 10^{-3}$ and the step time $\delta t = 2 \times 10^{-4}$. This solution will be denoted by $(U^n_{\text{ref}}, V^n_{\text{ref}})$ for which computations have been made with parameters equal to $\kappa = 1$, $\gamma = 0.5$ and $g_1 = g_2 = g = 1$.

2.1 Spatial error analysis

In order to check the accuracy in space of the scheme, solutions have been computed with various spatial steps, for the same time step $\delta t = 2.10^{-4}$ (see Tab. 1).
Let us denote these solutions by U^n_s for $\delta x_s = \delta y_s = 4.10^{-3}$ (for $s = 1$), 8.10^{-3} (for $s = 2$), $1.6\,10^{-2}$, $3.2\,10^{-2}$. Comparing each solution with the referent solution, the numerical error is calculated by

$$\text{err}(U_s)^2 = \sum_{n=1}^{N} ||U^n_{\text{ref}} - U^n_s||_2^2 \quad \text{for each} \quad s = 1, \ldots, 4.$$

Then, computing the ratios for each value of s,

$$\frac{\log(\text{err}(U_s)) - \log(\text{err}(U_{s-1}))}{\log(\delta x_s) - \log(\delta x_{s-1})}, \quad \text{and} \quad \frac{\log(\text{err}(V_s)) - \log(\text{err}(V_{s-1}))}{\log(\delta x_s) - \log(\delta x_{s-1})},$$

we get the spatial scheme order. The numerical results that have been given in Tab. 1 concern the fixed point iteration method. Similar results have been obtained for Newton method, which was not surprising. Indeed in our scheme, the only term involving the spatial mesh is the discrete Laplace operator which does not depend of the temporal approximation scheme.

s	Spatial step	Error	Order
0	4.0×10^{-3}	4.0×10^{-8}	
1	8.0×10^{-3}	2.0×10^{-7}	2.32
2	1.6×10^{-2}	8.4×10^{-7}	2.07
3	3.2×10^{-2}	3.4×10^{-6}	2.01

(a) Results for the 1st equation

s	Spatial step	Error	Order
0	4.0×10^{-3}	6.15×10^{-8}	
1	8.0×10^{-3}	3.07×10^{-7}	2.32
2	1.6×10^{-2}	1.29×10^{-6}	2.07
3	3.2×10^{-2}	5.22×10^{-6}	2.01

(b) Results for the 2nd equation

Table 1: Convergence for the fixed point iteration method

Without surprise, one obtains that our scheme seems to being at least second order accurate whatever the temporal approximation is chosen.

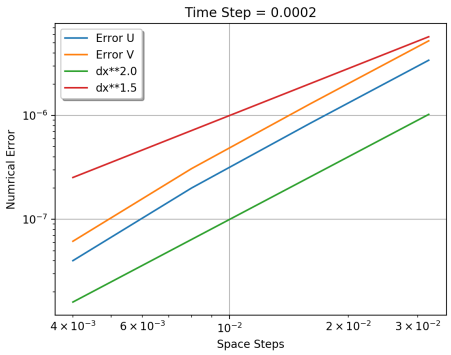

Figure 1: Convergence for the scheme using the fixed point iteration method

2.2 Error analysis in time

Following the convergence analysis in space, the temporal approximation is examined. In each direction, the spatial step has been fixed to $\delta x = \delta y = 2 \times 10^{-3}$. Then, the approximate solutions denoted here by U_s^n with various time steps : $\delta t_s = 4 \times 10^{-4}$, 8×10^{-4}, 1.6×10^{-3}, 3.2×10^{-3} (for each $s = 0, \ldots, 4$). Each solution U_s is compared with the referent solution, allowing to compute a global truncation error for each time step, by

$$\mathrm{err}(U_s^n)^2 = \sum_{n=1}^{N} ||U_{\mathrm{ref}}^n - U_s^n||_2^2, \quad \mathrm{err}(V_s^n)^2 = \sum_{n=1}^{N} ||V_{\mathrm{ref}}^n - V_s^n||_2^2.$$

s	Time step	Error	Order
0	4.0×10^{-4}	1.30×10^{-6}	
1	8.0×10^{-4}	4.30×10^{-6}	1.62
2	1.6×10^{-3}	1.06×10^{-5}	1.30
3	3.2×10^{-3}	1.98×10^{-4}	4.22

(a) Results for the 1st equation

s	Time step	Error	Order
0	4.0×10^{-4}	1.04×10^{-6}	
1	8.0×10^{-4}	3.22×10^{-6}	1.62
2	1.6×10^{-3}	7.96×10^{-6}	1.30
3	3.2×10^{-3}	2.52×10^{-5}	1.66

(b) Results for the 2nd equation

Table 2: $\ell^2(]0,T[;\ell^2(I))$-error behavior of the scheme using the fixed point iteration method

s	Time step	Error	Order
0	4.0×10^{-4}	9.88×10^{-9}	
1	8.0×10^{-4}	4.14×10^{-8}	2.06
2	1.6×10^{-3}	1.73×10^{-7}	2.06
3	3.2×10^{-3}	7.79×10^{-7}	2.17

(a) Results for the 1st equation

s	Time step	Error	Order
0	4.0×10^{-4}	1.47×10^{-8}	
1	8.0×10^{-4}	5.75×10^{-8}	1.97
2	1.6×10^{-3}	2.28×10^{-7}	1.99
3	3.2×10^{-3}	1.01×10^{-6}	2.140

(b) Results for the 2nd equation

Table 3: $\ell^2(]0,T[;\ell^2(I))$-error behavior of the scheme with the Newton method

The results confirm that the scheme with the fixed point iteration method is of order 1.5 (one obtains 1.6, see Tab. 2 and Fig. 2a), while the convergence of the scheme with Newton's method is quadratic (see Tab. 3 and Fig. 2b). Therefore, as it was expected, the rate of convergence of the Newton method is higher than those of the fixed–point iteration one. Moreover, from a computational point of view, the scheme using the Newton method is more efficient. One can also notice a curious result from Tab. 2 (last line for $\delta t = 3.2\,10^{-3}$), and also a change of slope in the error decrease (see Fig.2a). Indeed, the order of more than 4 is not significant caused by a too coarse time step.

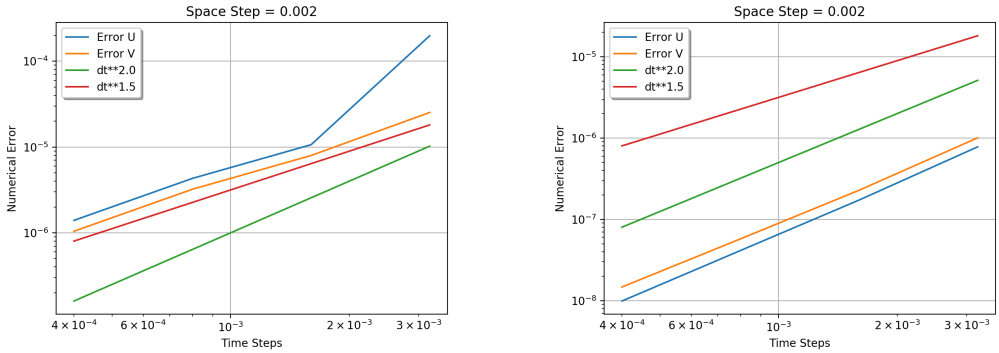

(a) Results with fixed point method

(b) Results with Newton's method

Figure 2: Convergence in time of the scheme

To conclude this section, the two algorithms that have been studied have the expected behavior and give suitable results.

3 Numerical experiments

This section is the main part of this work. Here, the results related to the qualitative behavior of the solution of the system (1) are given. First, one gathers the results concerning the Manakov case, then the generalized Manakov case.

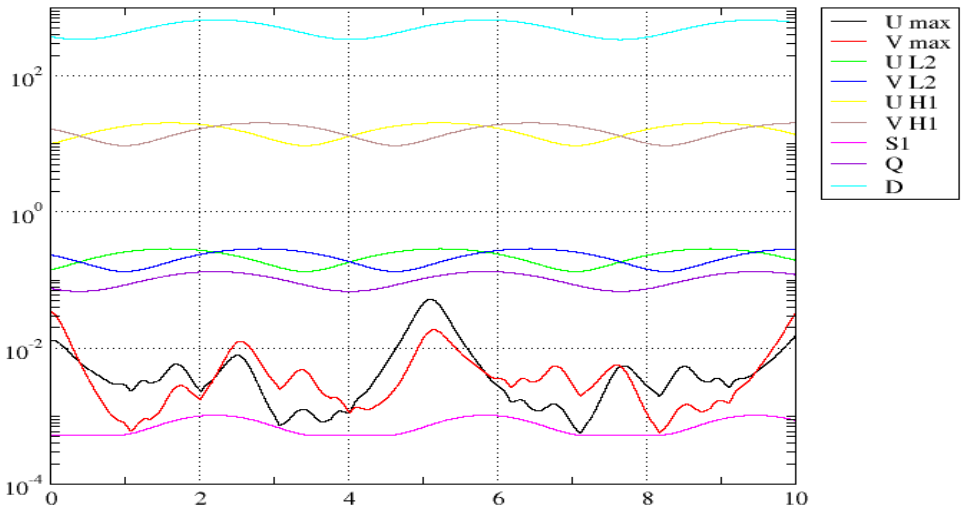

Figure 3: $||u||_{L^2}$ (green), $||v||_{L^2}$ (blue), $||\nabla u||^2_{L^2}$ (yellow), $||\nabla v||^2_{L^2}$ (brown), $||u||^2_{L^\infty}$ (black) and $||v||^2_{L^\infty}$ (red), $S_1(t)$ (magenta), $Q(t)$ (purple) et $D(t)$ (celestial blue) for initial condition (2) such that $(A, B) = (0.1, 0.2)$, $(\kappa, \gamma) = (1, 0.5)$ and $g_1 = g_2 = g = 1$.

3.1 The Manakov case

Numerical results are given in the Manakov case, i.e. when the coefficients of all nonlinear terms are equal. For the computations, the choice of nonlinear parameters value is $g_1 = g_2 = g = 1$, to keep more flexibility on the other parameters. Our results confirm the theoretical results given in [19]. In case of $\gamma < \kappa$ and an initial condition that verifies the condition $Q_{\max} < \frac{1}{2}||R||_2^2$, there exists a global solution for the system (1) (with $Q_{\max}$ being the upper bound of the density, R being a ground state solution of the stationnary equation $\Delta R - R + R^3 = 0$, $||R||_2^2 \approx (1.86255)\,\pi$, see [22]). According to our numerical results, four quantities stay bounded in time: the L^2 norm of the solution, the L^2 norm of its gradient and the L^∞ norm of the solution; also, the density $Q(t)$ is oscillating, but stays bounded. Moreover the semi–norm $D(t)$ does not blow up in finite time, that would mean that the solution of the system exists overall in time (see Fig. 3).

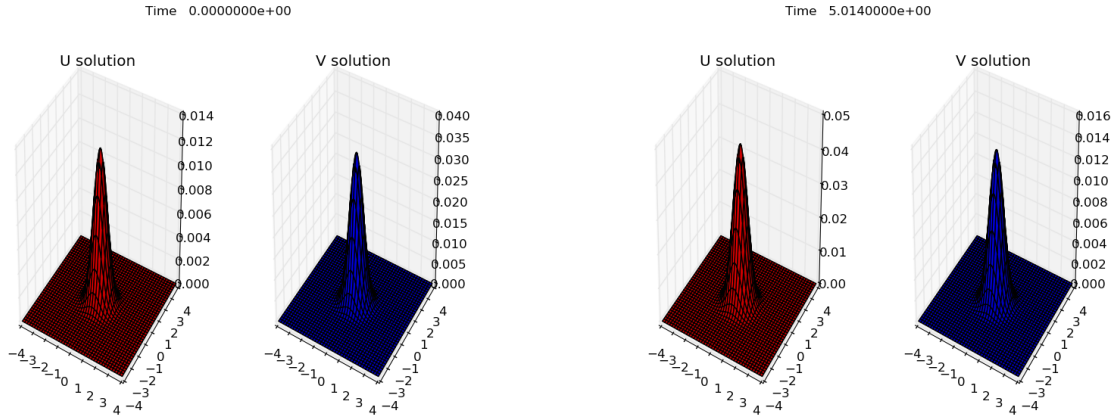

(a) the solution at time $t = 0.0$, $t = 5.0.14$

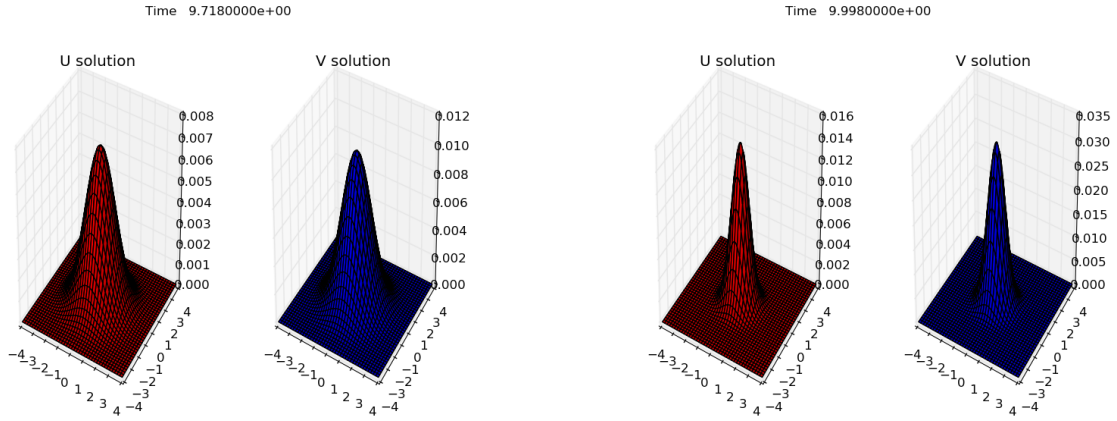

(b) the solution at time $t = 9.718$, $t = 10.0$

Figure 4: Modulus squared of the computed density (1st component in red, 2nd one in blue) at several times, in the Manakov case, for an initial condition (2) such that $(A, B) = (0.1, 0.2)$, $(\kappa, \gamma) = (1, 0.5)$ and $g_1 = g_2 = g = 1$.

Under the condition $\gamma < \kappa$ but using an initial condition such that $Q_{\max} \geq ||R||_2^2$, one knows that the solution does not exist after a finite time [19]. This result is illustrated by numerical computations which confirm that the L^2 norm of the gradient of the solution, the L^∞ norm of the solution and the quantity $D(t)$ grow infinitely over time; the solution blows up in finite time (see Fig. 5). The first Stokes variable S_1 is analytically conserved in time when all nonlinear coefficients are equals (the Manakov case). One can notice that the computations confirm this conservative behavior property over time (S_1 has a quasi flat magenta curve see Fig. 3). However, as soon as the initial condition is such that $\frac{1}{2}||R||_2^2 \leq Q_{\max} < ||R||_2^2$, no theoretical result exists, up to our knowledge. But, the numerical results reported at the fourth and fifth line of the table 4 seem to attest that the solution exists all time long (see also Fig. 8).

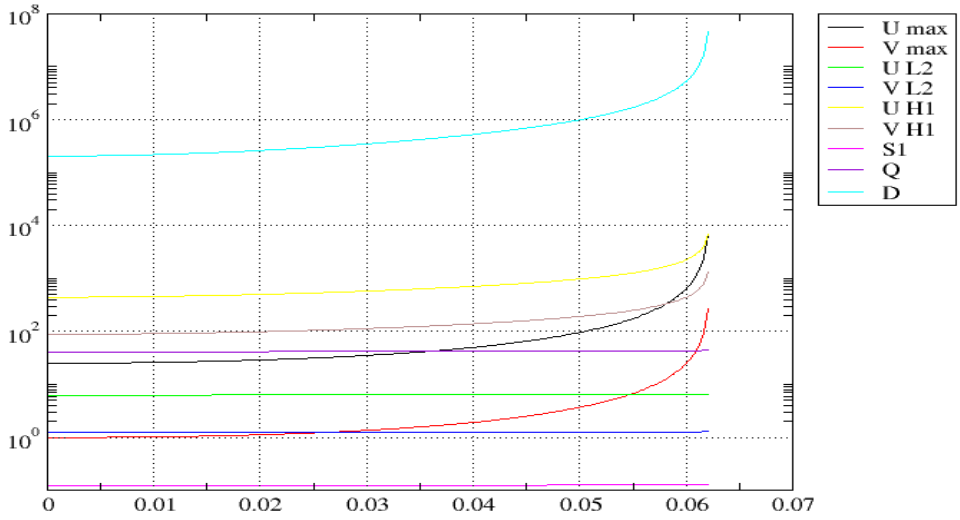

Figure 5: $||u||_{L^2}$ (green), $||v||_{L^2}$ (blue), $||\nabla u||^2_{L^2}$ (yellow), $||\nabla v||^2_{L^2}$ (brown), $||u||^2_{L^\infty}$ (black) and $||v||^2_{L^\infty}$ (red), $S_1(t)$ (magenta), $Q(t)$ (green) et $D(t)$ (celestial blue) for an initial condition (2) such that $(A, B) = (5, 1)$, $(\kappa, \gamma) = (1, 0.5)$ and $g_1 = g_2 = g = 1$.

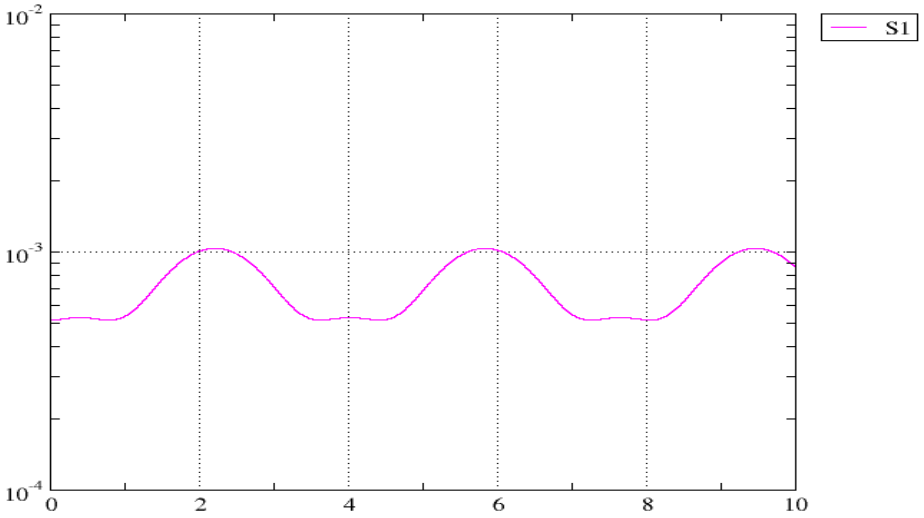

Figure 6: Behavior of S_1 versus time for initial condition (2) such that $(A, B) = (0.1, 0.2)$, $(\kappa, \gamma) = (1, 0.5)$ and $g_1 = g_2 = g = 1$.

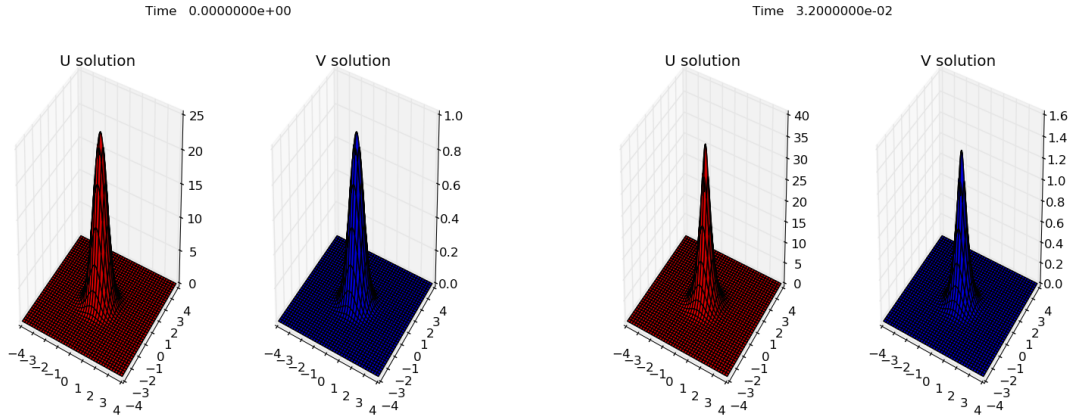

(a) the solution at time $t = 0.0$ et $t = 0.032$

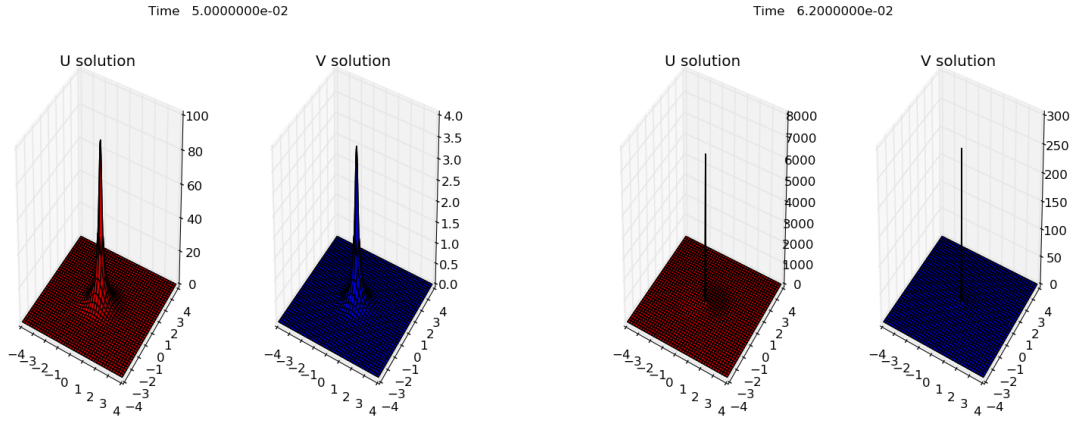

(b) the solution at time $t = 0.05$ et $t = 0.062$

Figure 7: Surfaces of the position density $|u(x,t)|^2$ (red) and $|v(x,t)|^2$ (blue) at time $t = 0.0$, $t = 0.032$ (upper row) and for $t = 0.05$, $t = 0.062$ (lower row) in the Manakov case, for the initial condition (2) such that $(A, B) = (5, 1)$, $(\kappa, \gamma) = (1, 0.5)$ and $g_1 = g_2 = g = 1$.

Thus, it is known that in the Manakov case, for $\gamma < \kappa$ and for initial conditions such as $Q_{\max} < \frac{1}{2}||R||_2^2$, the solution of the Cauchy problem exists globally, while for initial conditions for which $Q_{\max} \geq ||R||_2^2$, the solution can blow up in finite time. Nevertheless, the value of $Q_{\max}$ does not depend only on initial conditions but it also relies on the values of the linear parameters γ and κ. The table 4 provides informations in this case. The blow up time noted t^* depends on the initial condition and the parameters γ and κ in the Manakov case. The first and the second lines of this table indicate that for sufficiently small initial conditions and some values of γ and κ, the solution exists and does not blow up in finite time. However, for values γ and κ sufficiently large the solution can blow up in finite time (see third line). From the sixth to the ninth row of the table 4, configurations for which the value of $Q_{\max}$ exceeds $||R||_2^2$, are gathered: then the solution blows up in finite time. Finally, in Manakov case, a configuration of a global existence of the solution is reported at the tenth line of table 4 which corresponds to Fig. 3. Whereas another configuration with initial conditions with higher value of $Q_{\max}$ is

illustrated at the last line, and corresponds to figure 5. It is valuable to be able to know the behavior of the solution when $\frac{1}{2}||R||_2^2 < Q_{\max} < ||R||_2^2$. So, in this case, our numerical results show that the solution of the system seems to exist overall, according to the fourth line in the table 4 and the figures 8, 9.

No	$Q(0)$	κ	γ	ω	$Q_{\max}$	t^*
1	0.410	3	1	2.828	0.602	–
2	0.410	100	80	536	2.018	–
3	0.410	200	199.75	9.997	326.695	0.077
4	7.070	3	0.50	2.958	7.47	–
5	7.070	1	0.50	0.866	11.7	–
6	7.070	1	0.55	0.835	13.199	5.513
7	7.070	1	0.60	0.800	15.021	5.566
8	7.070	5	3.50	5.571	20.65	0.368
9	7.070	7	6	3.605	46	0.2252
10	0.075	1	0.5	0.866	0.133	–
11	40.841	1	0.5	0.866	80.127	0.062

Table 4: Blow up time according to initial conditions and linear parameters γ and κ in the Manakov case PT–symmetric; t^* is the computed value of the blow up time and $(-)$ means there is no blow up.

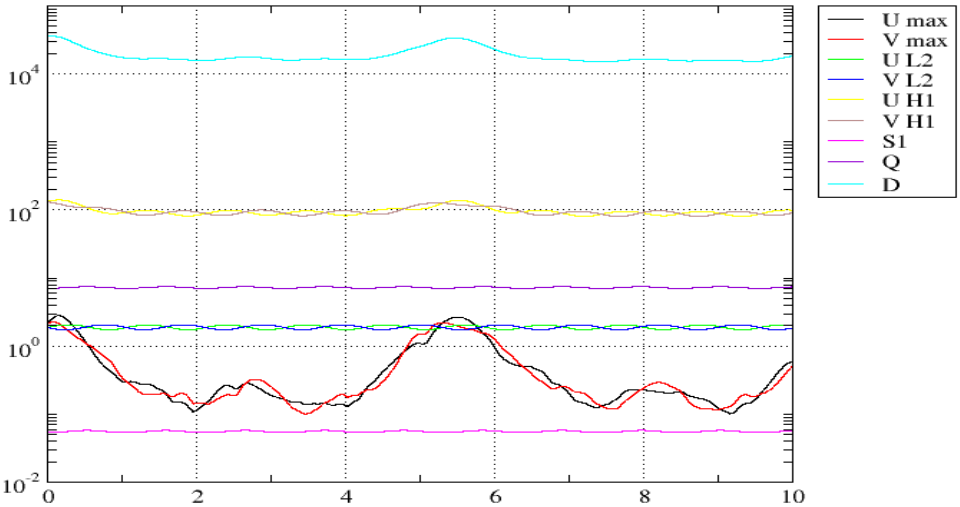

Figure 8: $||u||_{L^2}$ (green), $||v||_{L^2}$ (blue), $||\nabla u||_{L^2}^2$ (yellow), $||\nabla v||_{L^2}^2$ (brown), $||u||_{L^\infty}^2$ (black) and $||v||_{L^\infty}^2$ (red), $S_1(t)$ (magenta), $Q(t)$ (purple) and $D(t)$ celestial blue) for initial condition (2) such that $(A, B) = (1.5, 1.5)$, $(\kappa, \gamma) = (3, 0.5)$ and $g_1 = g_2 = g = 1$.

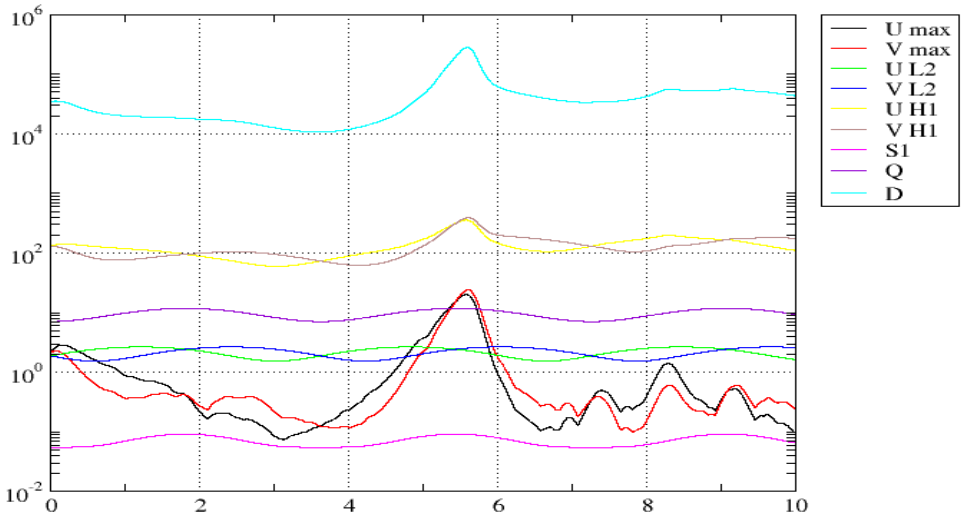

Figure 9: $||u||_{L^2}$ (green), $||v||_{L^2}$ (blue), $||\nabla u||^2_{L^2}$ (yellow), $||\nabla v||^2_{L^2}$ (brown), $||u||^2_{L^\infty}$ (black) and $||v||^2_{L^\infty}$ (red), $S_1(t)$ (magenta), $Q(t)$ (purple) et $D(t)$ (celestial blue) for initial condition (2) such that $(A, B) = (1.5, 1.5)$, $(\kappa, \gamma) = (1, 0.5)$ and $g_1 = g_2 = g = 1$.

3.2 The non Manakov case

When the coefficients of the nonlinear terms of the system (1) are not equal, the study of the blow up phenomenon in finite time has been studied (theoretically and numerically) in supercritical dimension by Dias (see [11]). Before this work, the qualitative study of the solution of the system (1) in the critical case was still an open problem. Subsequently, the model was address partially in the Manakov case, in the critical dimension by Pelinovsky (see [19]) and this result is illustrated by numerical results in this paper. For instance, there is not really any global result on this model in critical dimension as revealed in [17]. Here, numerical approximations are presented to show the global existence and blow up in finite time of the solution of the system in the critical dimension. For this group of tests, the model parameters are chosen as follows: $\kappa = 1$, $\gamma = 0.5$ and $g_1 = g_2 = 1 \neq g = 0.5$. But also to maintain the stability of the PT-symmetry, the option $\gamma < \kappa$ has been made [17]. Firstly, an initial condition was chosen and defined by (2) with $(A, B) = (0.1, 0.2)$. The results of these experiments are presented in Fig. 10 and 12. The L^2-norm and $L^\infty-$norm of the components of the solution, as well as the L^2-norm of its gradient are all bounded (see Fig. 10). Moreover, the density $Q(t)$ and the L^2-norm of the gradient of the solution, $D(t)$ remain bounded during the evolution over time of the solution. Furthermore, Fig. 10 brings to light that even if the coefficients of the nonlinear terms of (1) are not all equal, an initial condition can be suffisiently small for which the solution exists overall.

Moreover, keeping the same physical parameters for the model, a choice of an initial condition is made, defined by (2) with $(A, B) = (1, 3)$. Despite the limitations due to the boundary condition, the result of these experiments confirms that the system solution explodes in finite time (see Fig. 11 and 13). Indeed, the $L^\infty-$norm of the components of the solution and the

L^2-norm of the gradient of the components of the solution increase *infinitely* with a vertical tangent at a certain time (see Fig. 11).

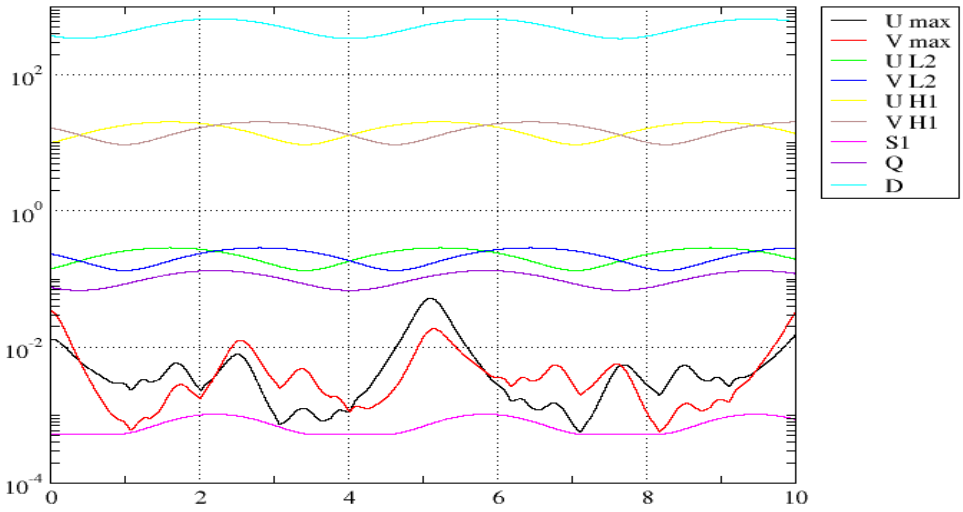

Figure 10: $||u||_{L^2}$ (green), $||v||_{L^2}$ (blue), $||\nabla u||^2_{L^2}$ (yellow), $||\nabla v||^2_{L^2}$ (brown), $||u||^2_{L^\infty}$ (black) and $||v||^2_{L^\infty}$ (red), $S_1(t)$ (magenta), $Q(t)$ (purple) et $D(t)$ (celestial blue) for initial condition (2) with $(A, B) = (0.1, 0.2)$, $(\kappa, \gamma) = (1, 0.5)$ and $g_1 = g_2 = 1 \neq g = 0.5$.

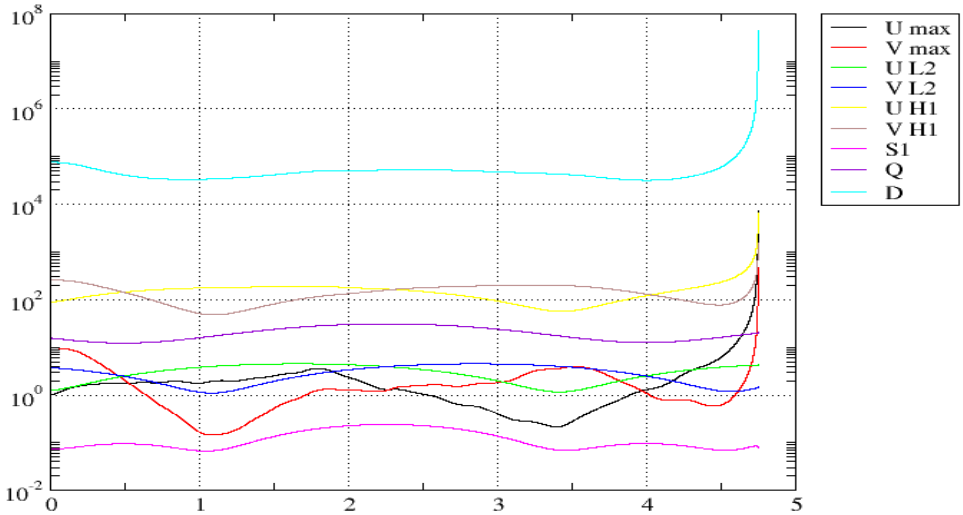

Figure 11: $||u||_{L^2}$ (green), $||v||_{L^2}$ (blue), $||\nabla u||^2_{L^2}$ (yellow), $||\nabla v||^2_{L^2}$ (brown), $||u||^2_{L^\infty}$ (black) and $||v||^2_{L^\infty}$ (red), $S_1(t)$ (magenta), $Q(t)$ (purple) et $D(t)$ (celestial blue) for initial conditions (2) with $(A, B) = (1, 3)$, $(\kappa, \gamma) = (1, 0.5)$ and $g_1 = g_2 = 1 \neq g = 0.5$.

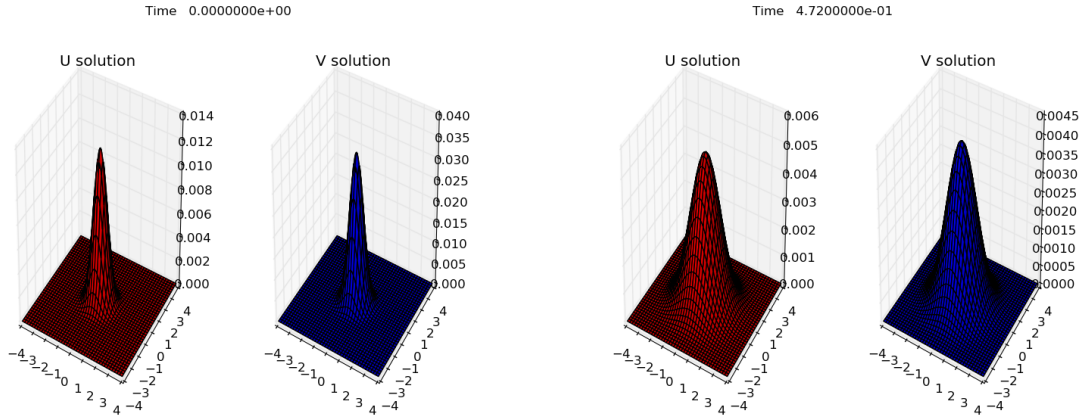

(a) the solution at time $t = 0.0$, $t = 0.0472$

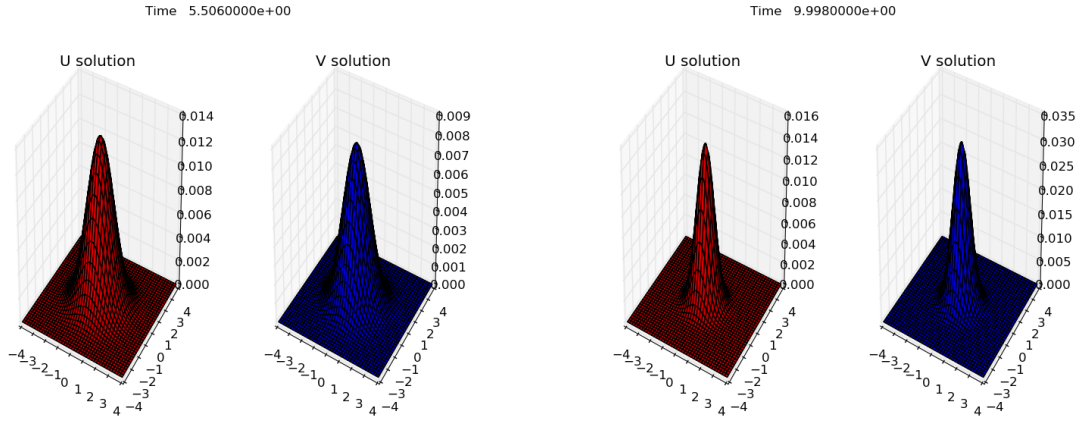

(b) the solution at time $t = 5.506$, $t = 9.998$

Figure 12: Surfaces of the position density $|u(x,t)|^2$ (red) and $|v(x,t)|^2$ (blue) at time $t = 0.0$, $t = 5.014$ (upper row) and for $t = 9.718$, $t = 10.0$ (lower row) in the general model case, for the inital condition (2) with $(A, B) = (0.1, 0.2)$, $(\kappa, \gamma) = (1, 0.5)$ and $g_1 = g_2 = g = 1$.

It is important to remind that all the previous computations were carried out on a delimited domain and with a Dirichlet boundary condition. But as one can see, all conserved quantities remain so, even when the boundary conditions influence the computed solution, which is, a priori, one of the limits of our approach. This is remarkable, so it is a conjecture, which will certainly be a subject for our future work.

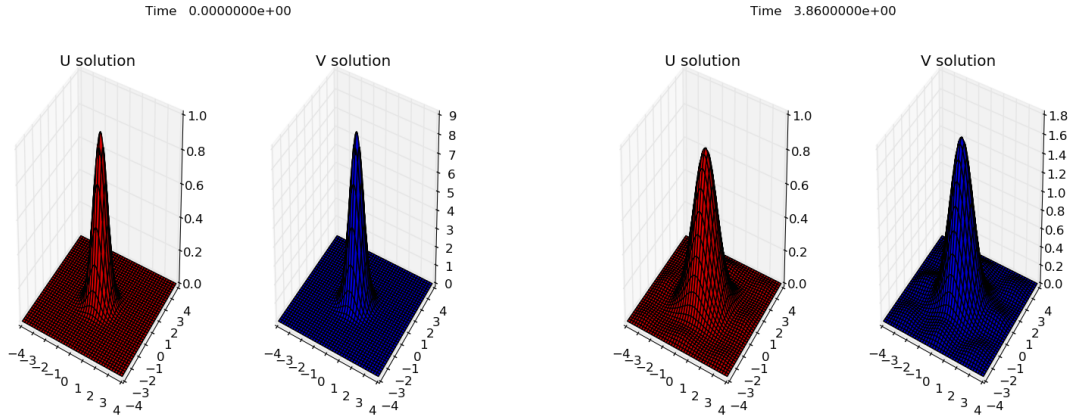

(a) the solution at time $t = 0.0$, $t = 3.86$

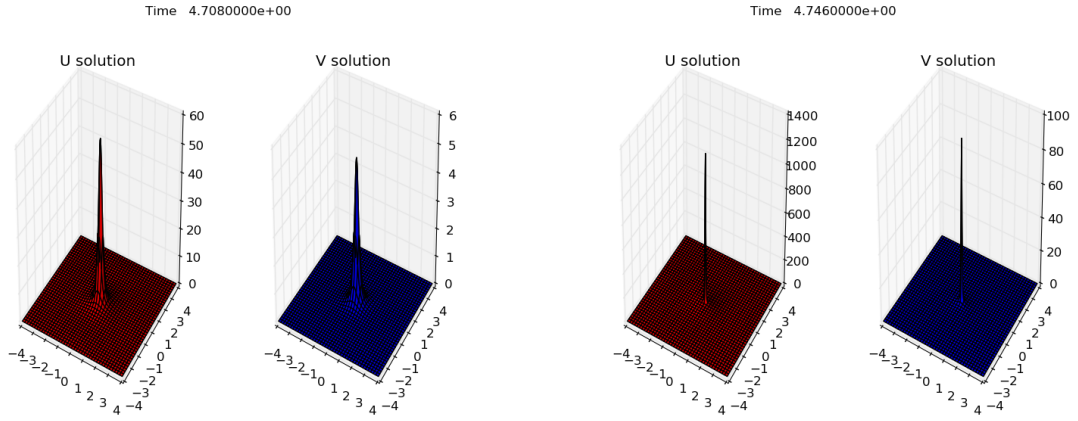

(b) the solution at time $t = 4.708$ et $t = 4.746$

Figure 13: Surfaces of the position density $|u(x,t)|^2$ (red) and $|v(x,t)|^2$ (blue) at time $t = 0.0$, $t = 3.860$ (upper row) and for $t = 4.708$, $t = 4.746$ (lower row) in the general model case, for initioal condition (2) with $(A, B) = (1, 3)$, $(\kappa, \gamma) = (1, 0.5)$ and $g_1 = g_2 = 1 \neq g = 0.5$.

Concluding remarks and perpectives

In this paper, we have numerically studied the behavior of the solution of the two coupled nonlinear Schrödinger equations, which one includes gains and the second includes losses. The numerical resolution of the system (1) has been made in a square domain by the second order centered finite different method and the scheme of Crank–Nicolson. Two iterative strategies are proposed the treat the non–linearity of the problem: the fixed point and the Newton method. An error analysis attest the numerical scheme is second order in space and it is 2nd order in time for the Newton method, and for the fixed point the scheme is 1.5 order in time. Numerical tests validate the existing theoretical results namely that for small initial conditions the solution exists globally over time. But also for large initial values conditions, the solution can blow up in finite time. Moreover, some experiments are made in order to study the influence of the

parameters of linear and nonlinear coupling, on the blow up time.

One of the unresolved problems in this paper concerns a theoretical estimate of the blow up time. For the coupled system with (1), defining absorbing boundary conditions or perfectly matched layers (PML) will be a subject for our future work. We will also need to improve our code, including the processing of the boundary conditions used with the numerical approximation domain, in order to be able to use it over longer periods of time. In addition, it will also be interesting to pass the code to dimension 3 to illustrate the theoretical results. Then, from 3D case, it would make it possible to speculate on results for the 2D case where there are still open problems.

Acknowledgements.

The authors are unanimously grateful to Prof. Ezzedine Zahrouni who suggested to us the topic of this paper. This is the main reason why, we wish to dedicate this paper in memory of Ezzedine Zahrouni. We will miss his fullness frienship and his capability of finding fruitful research topics. The authors are also pleased to acknowledge the Centre Commun de Calcul Intensif de l'Université des Antilles where the computational tests have been performed (see http://www.univ-antilles.fr/c3i).

References

[1] G.P. Agrawal, *Applications of Nonlinear Fiber Optics*, Optics and Photonics Series 2nd edition, Academic Press, Elsevier 2008.

[2] X. Antoine, C. Besse and S. Descombes, *Artificial boundary conditions for one–dimensional cubic nonlinear Schrödinger equations*. SIAM J. Numer. Anal. 43 (2006), no. 6, 2272–2293.

[3] V. A. Baskakov and A. V. Popov, *Implementation of transparent boundaries for numerical solution of the Schrödinger equation*. Wave Motion 14 (1991), no. 2, 123–128.

[4] C.M. Bender, *Making sense of non-Hermitian Hamiltonians*, Rep. Prog. Phys. **70** 947 (2007).

[5] C.M. Bender, B. Berntson, D. Parker and E. Samuel, *Observation of PT phase transition in a simple mechanical system*, Am. J. Phys. **81** 173 (2013).

[6] C.M. Bender and S. Borttcher, *Real spectra in non-Hermitian Hamiltonians having $\mathcal{PT}-$symmetry*, Phys. *Rev. Lett.* **80:24** (1998) 5243-5246.

[7] E. Destyl, S.P. Nuiro and P. Poullet, *On the global behavior of solutions of a coupled system of nonlinear Schrödinger equation*, Stud. Appl. Math. **138** (2017) 227–244.

[8] E. Destyl, S.P. Nuiro, D.E. Pelinovsky and P. Poullet, *Coupled pendula chains under parametric $\mathcal{PT}$-symmetric driving force*. Phys. Lett. A **(381)** 46 (2017) 3884–3892.

[9] E. Destyl, S.P. Nuiro and P. Poullet, *Critical blow up in coupled Parity-Time-symmetric nonlinear Schrödinger equations*. AIMS Math. Vol. 2 **(1)** (2017) 195–206.

[10] E. Destyl, Modélisation et analyse de systèmes d'équations de Schrödinger non linéaire, *Thèse de doctorat de l'Universté des Antilles*, 28 septembre 2018, Pointe-à-Pitre, Guadeloupe.

[11] J.-P. Dias, M. Figueira, V.V. Konotop and D.A. Zezyulin, *Supercritical blow up in coupled parity-time-symmetric nonlinear Schrödinger equations*. Stud. Appl. Math. **133** (2014) 422–440.

[12] J.P Dias, M. M. Figueira and V. V. Konotop, *The Cauchy problem for coupled nonlinear Schrödinger equations with linear damping: local and global existence and blow up of solutions*. Chin. Ann. Math. **37B(5)** (2016) 665–682.

[13] L. Di Menza, *Transparent and absorbing boundary conditions for the Schrödinger equation in a bounded domain*. (English summary) Numer. Funct. Anal. Optim. **18** (1997) no. 7-8 759–775.

[14] R. Driben and B.A. Malomed, *Stability of solitons in parity-time-symmetric couplers*. Opt. Lett. **36**:22, (2011) 4323–4325.

[15] M.S. Ismail and T.R. Taha, *Numerical simulation of coupled nonlinear Schödinger equation*. Math. Comput. Simul. **56** (2001) 547-562.

[16] A. Jüngel and R.-M. Weishäupl, *Blow up in two-component nonlinear Schrödinger systems with an external driven field*, Math. Models Methods Appl. Sci. **23** (2013) 1699–1727.

[17] V. V. Konotop, J. Yang and D.A. Zezyulin, *Nonlinear waves in PT–symmetric systems*. Rev. Mod. **88:3** (2016) 035002(59).

[18] F. Linares and G. Ponce, *Introduction to Nonlinear Dispersive Equations*. Springer, LLC 2009.

[19] D.E. Pelinovsky, D.A. Zezyulin and V.V. Konotop, *Global existence of solutions to coupled PT–symmetric nonlinear Schrodiger equations*. Int. J. Theor. Phys. **54** (2015) 3920–3931.

[20] C. Sulem and P-L Sulem, *The Nonlinear Schrödinger Equation*, Springer, New-York, 1999.

[21] T.R. Taha and M.J. Ablowitz, *Analytical and numerical aspects of certain nonlinear evolution equations II. Numerical nonlinear Schrödinger equation*. J. Comp. Phys. **55** (2006) 203–230.

[22] M.I. Weinstein, *Nonlinear Schrödinger equations and sharp interpolation estimates*. Commun. Math. Phys. **87** (1983) no. 4 567–576.

[23] C. Zheng, *A perfectly matched layer approach to the nonlinear Schrödinger wave equations*. J. Comput. Phys. **227** (2007) no. 1 537–556.